Journal of Neuropathology and Experimental Neurology

Vol. 54, No. 5
September, 1995
pp. 657–663

Absence of Abnormal Hyperphosphorylation of Tau in Intracellular Tangles in Alzheimer's Disease

WILLIAM BONDAREFF, PH.D., M.D., CHARLES R. HARRINGTON, PH.D.,
CLAUDE M. WISCHIK, M.D., PH.D., DOUGLAS L. HAUSER, B.A., AND MARTIN ROTH, M.D., SC.D.

Abstract. Adult human nerve cells contain tau protein, a phosphorylated microtubule-associated protein, that is hyperphosphorylated in the fetus and in patients with Alzheimer's disease. Hyperphosphorylation, which diminishes the microtubule-binding capacity of tau, destabilizes microtubules and may enhance the formation of paired helical filaments that constitute neurofibrillary tangles in Alzheimer's disease. Here, we use phosphorylation-dependent anti-tau antibodies to detect specific epitopes that characterize hyperphosphorylated tau. Our demonstration of intracellular tangles containing full-length tau that are not immunolabeled by these antibodies suggests that hyperphosphorylation of tau is not obligatory in the formation of neurofibrillary tangles in Alzheimer's disease.

Key Words: Alzheimer's disease; Hyperphosphorylation; Neurofibrillary tangles; Tau.

INTRODUCTION

A close relationship between neurofibrillary tangles (NFT) and dementia in Alzheimer's disease (AD) has been established (1–5). Neurofibrillary tangles, which are well developed in pyramidal neurons of hippocampus, are composed of densely packed bundles of microscopic-size filaments, made up largely of paired helical filaments (PHF) (6, 7). Paired helical filaments are known to contain tau protein as an integral constituent (8, 9). In addition to NFT, PHF occur in neuropil threads and dystrophic neurites associated with plaques (10).

A monoclonal antibody, Alz50, recognizes pathological PHF-containing structures and certain tangle-free neurons, presumably before the formation of NFT (11, 12). On immunoblots, it recognizes all human tau isoforms in normal adult and fetal brains (13, 14) and A68, a mixture of sarkosyl-insoluble tau proteins with apparent molecular mass of 60–68 kDa prepared from brains of AD patients (15). Whereas normal adult tau protein is phosphorylated to a limited extent (2–3 mols phosphate per mol tau) in postmortem brain, A68 is abundantly phosphorylated at multiple sites, including serine 202 and serine 396, which are not phosphorylated in normal adult, autopsy-derived tau (15, 16). Phosphorylation of these two sites also occurs in fetal tau (16, 17).

Phosphorylated residues that have been identified in fetal and PHF tau include serine 202, serine 235, serine 262, serine 396, serine 404, threonine 231 and threonine 181 (18, 19). With the exception of serine 202 and serine 396, these sites have been found to be partially phosphorylated in normal adult tau (19). In PHF tau, these sites are abundantly phosphorylated (19) and PHF tau can, therefore, be said to be abnormally phosphorylated (i.e. hyperphosphorylated). Hyperphosphorylated tau, i.e. that which is fully phosphorylated at serine 202 and serine 396, is also known as A68 (20).

One possible consequence of hyperphosphorylation of tau is the loss of normal microtubule-binding capacity and, consequently, the destabilization of microtubules (21, 22). As it has been claimed that A68 proteins are essential building blocks of PHF (15), it has been proposed that a second consequence of abnormal hyperphosphorylation is the facilitation of PHF formation. This proposal seems incongruous with the formation of PHF-like polymers from tau fragments containing only the repeat region (23, 24) and full-length non-phosphorylated recombinant tau (25). It could be speculated, therefore, that phosphorylation of serine 202 and/or serine 396 is not obligatory for PHF formation *in vivo*. The existence, demonstrated here, of intracellular NFT with full-length tau unlabeled (or in large part unlabeled) by phosphorylation-dependent antibodies that otherwise recognize serine 202 and serine 396 suggests that phosphorylation at these sites is not an essential prerequisite for PHF formation.

MATERIALS AND METHODS

Segments of medial temporal lobe containing the hippocampus were obtained from 11 patients (Table 1) with well-documented AD. The diagnosis in each case satisfied NINCDS/ADRDA criteria for definite AD (26). The specimens were fixed in methanol containing 5% acetic acid, embedded in paraffin wax, and sectioned serially at 15 μm as has been described (27). The sections were stained with Congo red (28) and immunolabeled with an anti-tau antibody. They were incubated

From the Department of Psychiatry and the Behavioral Sciences (WB, DLH), Division of Geriatric Psychiatry, University of Southern California Medical School, Los Angeles, and the Cambridge Brain Bank Laboratory (CRH, CMW, MR), Department of Psychiatry, MRC Centre, Cambridge, United Kingdom.

Supported in part by the Della Martin Foundation (Los Angeles), Sankyo Co., LTD (Tokyo) and the Charles Wolfson Charitable Trust (London).

Correspondence to: W. Bondareff, M.D., Ph.D., Department of Psychiatry and Behavioral Sciences, Division of Geriatric Psychiatry, University of Southern California Medical School, MOL 202, Los Angeles, CA 90033.

TABLE 1
Numbers of AT8-positive and AT8-negative Intracellular Tangles per mm² Hippocampus (Area CA1) and Clinical Characteristics of Patients with Probable Alzheimer's Disease

Specimen	Age	Sex	Dur	PMI	Intracellular tangles AT8+	Intracellular tangles AT8−
40	76	M	4	un	46.7	6.2 (12)
64	91	F	7	6	5.6	6.1 (52)
65	78	M	8	10	37.6	0 (0)
75	72	M	10	33	50.3	0 (0)
77	75	F	9	14	6.5	3.5 (35)
78	67	F	7	50	31.4	7.9 (20)
80	84	M	3	11	35.3	6.2 (15)
81	84	F	10	15	63.9	0.9 (1)
96	un	M	un	un	17.1	0 (0)
100	92	F	6	12	37.0	1.8 (5)
104	76	M	4	17	78.9	1.8 (2)

Age = age at death in years.
Dur = duration of dementia in years.
PMI = Postmortem Interval.
un = Unknown.
( ) = % total intracellular tangles.

overnight with the primary antibody (diluted 1:20 with phosphate-buffered saline, PBS), washed with PBS, and incubated for 1 hour with a fluorescein isothiocyanate (FITC)-conjugated anti-mouse immunoglobulin (used with monoclonal primary antibodies) or a FITC-conjugated anti-rabbit immunoglobulin (used with polyclonal antibodies). The sections were mounted on glass slides in Citifluor (Ted Pella, Inc. Redding, CA). The method of immunolabeling has been described (29).

Antibodies

The anti-tau antibodies used were: AT8, AT180, and AT270 (provided by Innogenetics N.V., Ghent, Belgium); SMI31 (Sternberger Monoclonals, Baltimore, MD); Alz50 (provided by Dr. Peter Davies); and BR133.

SMI31 has been shown to recognize a phosphorylation-dependent site between serine residues 396 and 404 (30). AT8 immunoreactivity depends upon phosphorylation of serine 202 (17). Other phosphorylation-dependent antibodies, AT270 and AT180, recognize epitopes requiring phosphorylation at threonine 181 and threonine 231, respectively (19). Part or all of the epitope recognized by Alz50 has been demonstrated in amino acid sequence 2–10 of tau protein and appears not to be phosphorylation-dependent (31), although Alz50 has also been shown to recognize a phosphatase-sensitive epitope (32). BR133 is a polyclonal antibody raised against amino acids 1–16 (33). These antibodies and their epitopes are summarized in Figure 1.

Confocal Microscopy

Sections stained with Congo red and immunolabeled with an anti-tau antibody were analyzed with a confocal microscope. The two fluorescence images, when superimposed, produced red and yellow images corresponding, respectively, to Congo red-stained and FITC-labeled objects, the former being more or less red depending on the relative amount of the FITC-labeled epitope present.

Sections were visualized at an initial magnification of 200–600× with a Nikon epifluorescence microscope equipped with 20/0.75 and 60/1.4 (oil immersion) planapochromatic objective lenses. Selected microscopic fields were then scanned with an MRC-600 laser scanning confocal microscope imaging system (Bio-Rad, Cambridge, MA). The system was equipped with an argon laser and high sensitivity 488 nm and 514 nm exciter filters. The emission spectra from the excited fluorophores were passed to photomultipliers, viewed on a monitor and photographed.

RESULTS

Both intra- and extracellular NFT are stained with Congo red (27), a diazo dye used in neurohistology. When viewed with a fluorescence microscope, intracellular NFT appear as densely packed bundles of intracytoplasmic filaments emitting a bright red fluorescence. These Congo red-labeled intracellular NFT appeared as brightly fluorescent objects in the red fluorophore-visualizing channel (514 nm exciter filter) of the laser scanning confocal imaging system (Fig. 2C, solid arrow). In the green fluorophore-visualizing channel (488 nm exciter filter) they were barely visible (Fig. 2B, solid arrow). Intracellular NFT that are stained with Congo red and not immunolabeled appear red when the two channel images are superimposed (Fig. 2A, solid arrow). Intracellular

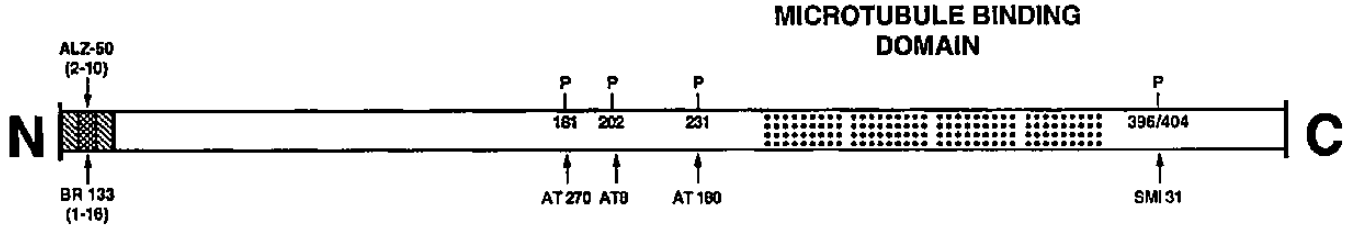

1

Fig. 1. Diagram of the longest human tau protein isoform. Phosphorylation sites are indicated by P. When known, the loci of epitopes recognized by antibodies used in this study are identified.

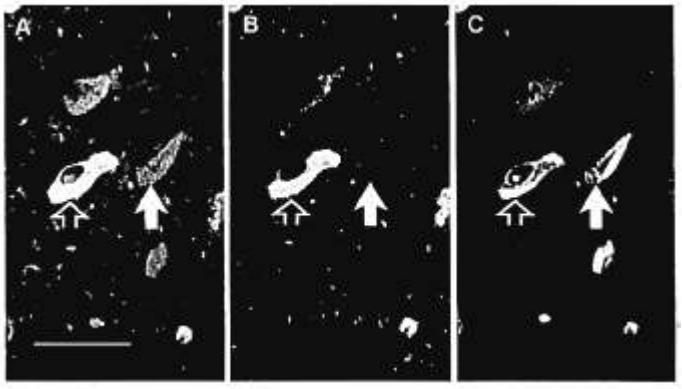

Fig. 2. Confocal microscope images of intracellular tangles in sections of hippocampal pyramidal neurons incubated with FITC-tagged AT8 and stained with Congo red. A. Merged image resulting from the superimposition of 488 nm and 514 nm channel images. The red intracellular tangle, not immunolabeled with AT8, is indicated by a closed arrow; the immunolabeled tangle is yellow (open arrow). B. In the 488 nm channel an intracellular tangle, not immunolabeled by AT8, is barely visible (closed arrow); an intracellular tangle immunolabeled by AT8 is clearly visible (open arrow). C. In the 514 nm channel intracellular tangles are clearly visible, brightly fluorescent images (arrows). Bar = 50 μm.

NFT that are stained with Congo red and simultaneously immunolabeled with a FITC-tagged anti-tau antibody had a similar structure but emitted a red-yellow fluorescence when viewed with a fluorescence microscope due to the combined presence of red (Congo red) and green (FITC) fluorophores. The NFT appeared more or less yellow depending upon the relative amounts of the two fluorophores. They appeared with variable brightness when viewed in either the 514 nm (Fig. 2C, open arrow) or 488 nm (Fig. 2B, open arrow) channel of the confocal microscope depending on the relative amounts of Congo red and FITC. When the 514 nm and 488 nm channel images were merged, the original color was captured (Fig. 2A, open arrow). In no case could an intracellular NFT be identified that emitted a green fluorescence, which would be indicative of antibody labeling in the absence of Congo red staining.

In specimens stained with Congo red and immunolabeled with FITC-tagged AT8, SMI31, Alz50, AT180, or AT270, intracellular NFT usually emitted a bright yellow fluorescence in the fluorescence microscope. A small percentage of such intracellular NFT emitted a bright red fluorescence, indicating a total, or virtually total, lack of immunolabeling with the above anti-tau antibodies. For example, the absence of immunolabeling of intracellular NFT that had also been stained with Congo red is illustrated in Figure 3. While no immunolabeling with SMI31 or Alz50 is seen in the 488 nm channel (Fig. 3C, D), the Congo red-stained NFT are clearly seen in the 514 nm channel (Fig. 3E, F) of the confocal microscope. The composite, merged images are seen in Figure 3A and B.

The numbers of Congo red-stained intracellular tangles that failed to immunolabel with AT8 were counted in area CA1 of the hippocampus and expressed both as the mean value per mm² and as a percentage of the total number of intracellular tangles. As the numbers of neurons that failed to immunolabel with AT8 were similar to those failing to immunolabel with SMI31, Alz50, AT180, or AT270, data are presented only for AT8 (Table 1). No significant correlations were found between the number or the proportion of AT8-negative neurons and age, sex, duration of dementia, or postmortem interval (PMI).

In specimens stained with Congo red and immunolabeled with BR133 all intracellular NFT emitted a bright yellow fluorescence in the fluorescence microscope. In no case was it possible to demonstrate an intracellular NFT emitting only a red fluorescence. In the confocal microscope, 488 nm (Fig. 4A) and 514 nm (Fig. 4B) channel images were virtually identical and the merged images (Fig. 4C) were essentially yellow.

DISCUSSION

These findings suggest the existence of a small population of intracellular NFT that stain with Congo red but fail to immunolabel with antibodies against specific phosphorylation-dependent epitopes. Two of these epitopes, which are typically recognized by AT8 and SMI31, have been demonstrated in fetal tau but are not detectable (in postmortem brain) in normal adult tau (reviewed in 34). They typically occur in intracellular PHF and are characteristic of hyperphosphorylated tau (A68) proteins (15). Similarly, a small percentage of Congo red-stained intracellular NFT fail to label with Alz50 (Fig. 3D). Because Alz50 has been shown to recognize a non-phosphorylated epitope in the amino acid sequence containing residues 2–10 (31), the lack of Alz50 immunolabeling might suggest the loss of the N-terminal region of the tau molecule. Alternatively, it is possible that unidentified conformational changes to the molecule might make the N-terminal epitope inaccessible to Alz50. Additionally, an unidentified sequence(s) or conformation not contained in residues 2–10 might contribute to the epitope recognized in intracellular NFT (35).

Because all intracellular NFT are immunolabeled by BR133 (Fig. 4), an antibody that recognizes an epitope within amino acid sequence 1–16 (33), our findings suggest that loss of the amino terminus of tau is not responsible for the failure of a small population of intracellular NFT to label with Alz50 or AT8. This would imply that conformational changes associated with the absence of AT8 immunoreactivity may also be responsible for the loss of Alz50 immunoreactivity. It has been demonstrated that phosphorylation can produce conformational changes in normal tau (36).

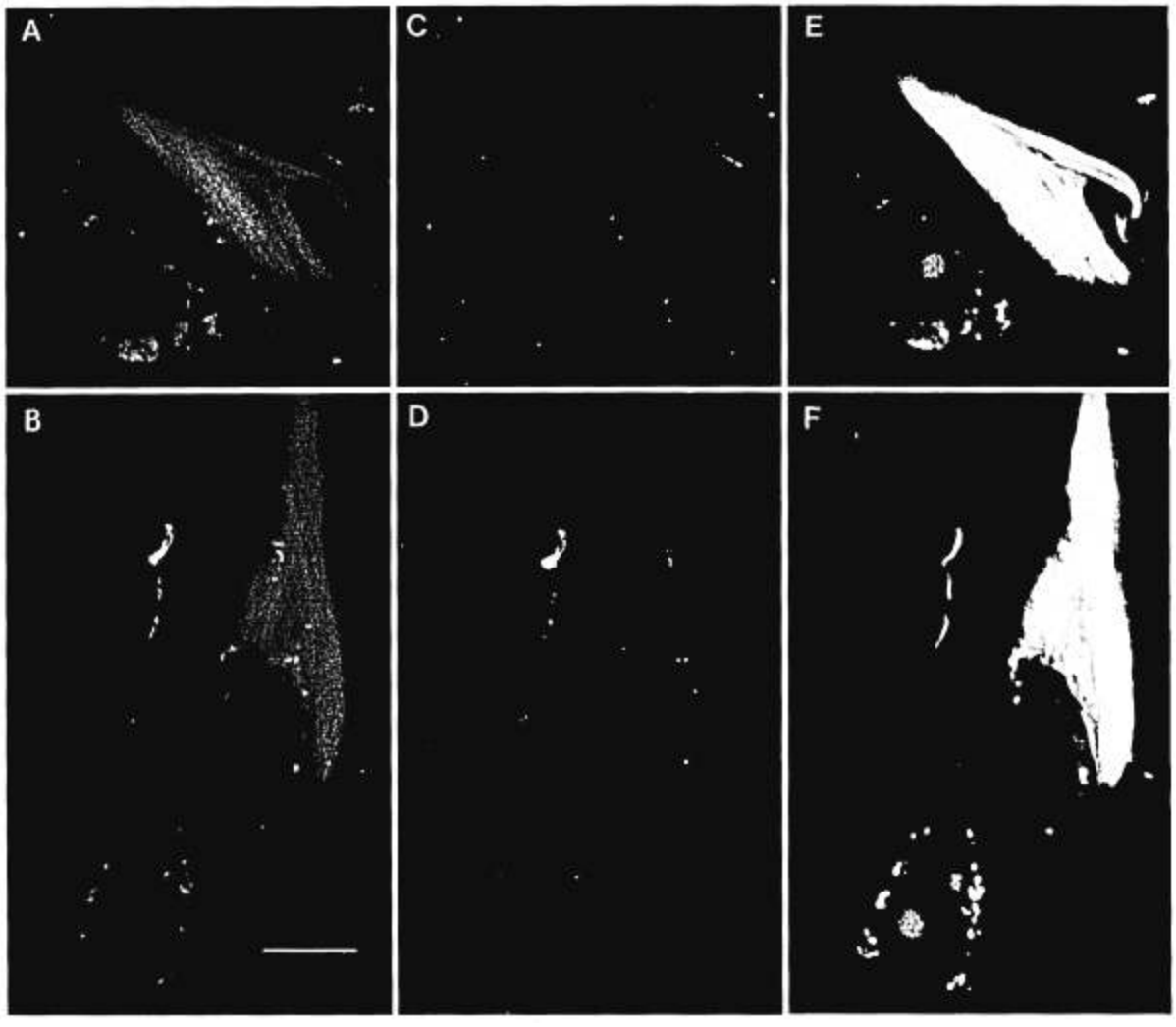

Fig. 3. Confocal microscope images of intracellular tangles in sections incubated with FITC-tagged SMI31 or FITC-tagged Alz50 and stained with Congo red. A. SMI31 and Congo red, merged image. B. Alz50 and Congo red, merged image. C. SMI31 and Congo red, 488 nm channel. D. Alz50 and Congo red, 488 nm channel. E. SMI31 and Congo red, 514 nm channel. F. Alz50 and Congo red, 514 nm channel. Bar = 10 μm.

In excisional biopsy specimens of human brain obtained during surgery (37) and in fresh rat brain (38), PHF tau, fetal tau, and normal adult human tau appear to be phosphorylated at similar phosphorylation sites including serine 202, serine 396, threonine 181, and threonine 231. Because these sites are more likely to remain phosphorylated in PHF tau than in normal adult tau in postmortem specimens, it has been suggested that hyperphosphorylation of PHF tau results from the downregulation of certain protein phosphatases in AD (37). It might also be suggested that variations in the immunoreactivity of phosphorylation-dependent epitopes of PHF tau, as reported here, might reflect variations in PMI. However, we failed to find statistically significant correlations between PMI and the number or proportion of unlabeled intracellular NFT (Table 1), suggesting, instead, the presence of a small population of NFT that are not phosphorylated at sites usually phosphorylated in PHF tau.

Our findings suggest that hyperphosphorylation of tau need not be an obligatory prerequisite for the formation of NFT. Although the metabolic process(es) underlying the phosphorylation of tau in intracellular NFT is not known, we would speculate that the accumulation of non-hyperphosphorylated tau into at least some PHF is consistent with our findings. There is no evidence of dephosphorylation of tau after being accumulated into PHF *in vivo*, although this has been demonstrated *in vitro* (17) and might contribute to the pool of normal tau from which PHF are formed. It seems unlikely that tau is dephosphorylated after NFT formation because the intracytoplasmic phosphatases would be expected to com-

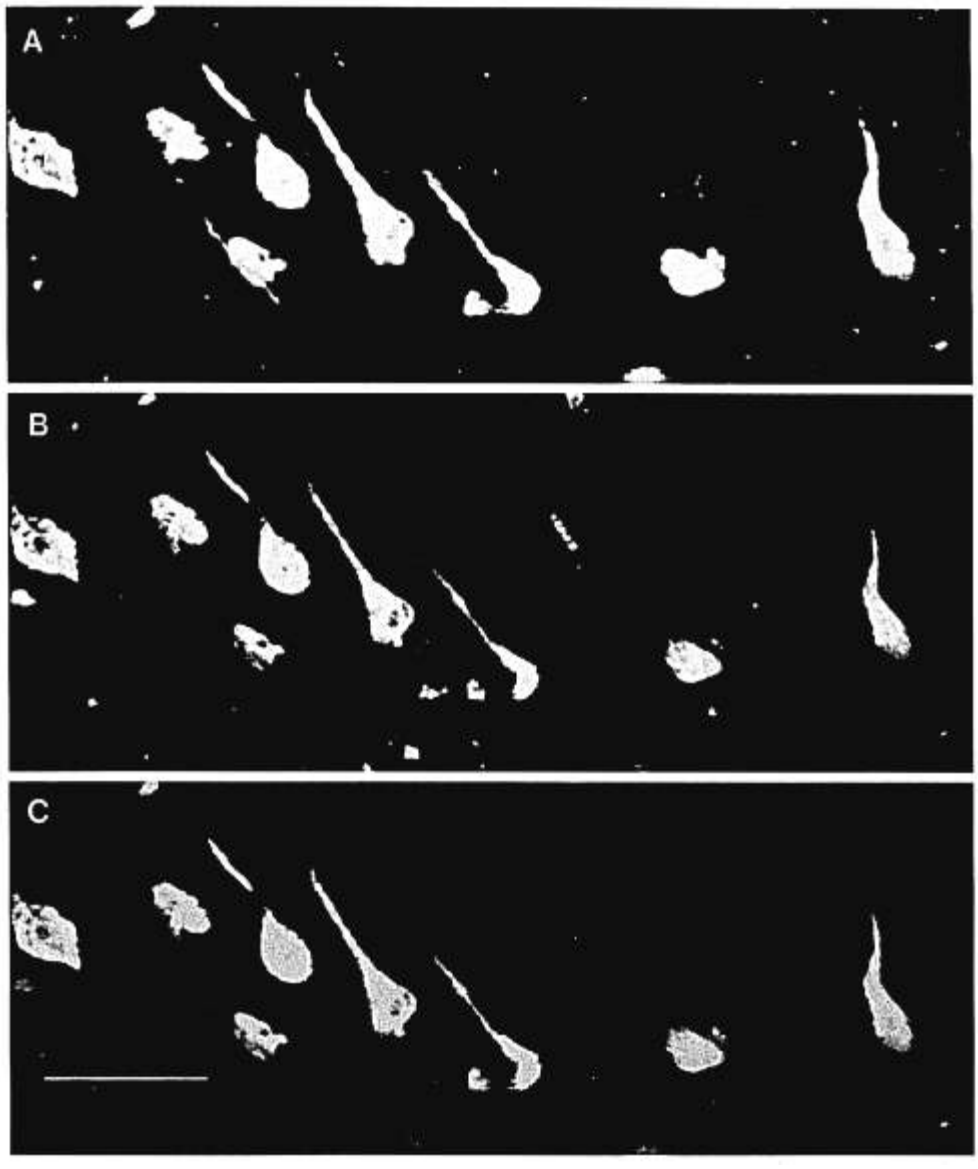

Fig. 4. Confocal microscope images of intracellular tangles immunolabeled with FITC-tagged BR133 and stained with Congo red. A. 488 nm channel. B. 514 nm channel. C. Merged image. Bar = 50 μm.

mence their action at the surface of the NFT prior to acting on internal filaments; image reconstruction by confocal microscopy gives no evidence of layers with different degrees of phosphorylation in any NFT.

The demonstration of NFT composed of little or no hyperphosphorylated tau argues against the necessity of abnormal phosphorylation for PHF assembly in AD (15, 17). It is, however, consistent with recent findings showing that only a minority of PHF are hyperphosphorylated in AD and that hyperphosphorylation inhibits the binding of tau to itself in the formation of tau complexes (39, 40). Our findings suggest that hyperphosphorylation of PHF tau can be seen as a variable secondary event that occurs after PHF begin to accumulate in the somatodendritic compartment of affected neurons.

The physical properties of tau depend upon its state of phosphorylation (36), and hyperphosphorylation has been shown to result in a decreased capacity to bind tubulin and stabilize microtubules (21, 22, 41–43). Indeed, it is conjectured that hyperphosphorylation of tau leads to a loss of microtubular integrity and failure of intracellular transport systems and that this is associated with neurofibrillary pathology and neuronal death in AD (44, 45).

Hyperphosphorylation of tau may also promote PHF formation in AD (15, 23, 24, 41). However, our results from this and other studies (39, 40) indicate that it may

not be a necessary prerequisite of PHF formation. The results of recent studies showing only minor abnormalities in tau-deficient mice (46) also point to the improbability that hyperphosphorylation of tau in PHF contributes directly to the process of neuronal death in AD.

ACKNOWLEDGMENTS

We are grateful to Dr. Peter Davies (Albert Einstein College of Medicine, New York) for providing Alz50 and to Dr. E. Vanmechelen (Innogenetics, Ghent) for providing AT8, AT180, and AT270.

REFERENCES

1. Wilcock GK, Esiri MM. Plaques, tangles and dementia: A quantitative study. J Neurol Sci 1982;56:343–56
2. McKee AC, Kosik KS, Kowall NW. Neuritic pathology and dementia in Alzheimer's disease. Ann Neurol 1991;30:156–65
3. Arriagada PV, Growdon JH, Hedley-White ET, Hyman BT. Neurofibrillary tangles but not senile plaques parallel duration and severity of Alzheimer's disease. Neurology 1992;42:631–9
4. Berg L, McKeel DW Jr, Miller JP, Baty J, Morris JC. Neuropathological indexes of Alzheimer's disease in demented and nondemented persons aged 80 years and older. Arch Neurol 1993;50: 349–58
5. Bondareff W, Mountjoy CQ, Wischik CM, Hauser DL, LaBree LD, Roth M. Evidence of subtypes of Alzheimer's disease and implications for etiology. Arch Gen Psychiatry 1993;50:350–6
6. Kidd M. Paired helical filaments in electron microscopy of Alzheimer's disease. Nature 1963;197:192–3
7. Terry RD, Gonatas NK, Weiss M. Ultrastructural studies in Alzheimer's presenile dementia. Am J Pathol 1964;44:669–97
8. Wischik CM, Novak M, Thogersen HC, et al. Isolation of a fragment of tau derived from the core of the paired helical filament of Alzheimer disease. Proc Natl Acad Sci USA 1988;85:4506–10
9. Kondo J, Honda T, Mori H, Hamada Y, Miura R, Ogawara M, Ihara Y. The carboxyl third of tau is tightly bound to paired helical filaments. Neuron 1988;1:827–34
10. Braak H, Braak E, Grundke-Iqbal I, Iqbal K. Occurrence of neuropil threads in the senile human brain and in Alzheimer's disease: A third location of paired helical filaments outside of neurofibrillary tangles and neuritic plaques. Neurosci Lett 1986;65:351–5
11. Wolozin BL, Pruchniki A, Dickson DW, Davies P. A neuronal antigen in the brains of Alzheimer patients. Science 1986;232: 648–50
12. Hyman BT, Van Hoesen GW, Wolozin BL, Davies P, Kromer BA, Damasio AR. Alz-50 antibody recognizes Alzheimer-related neuronal changes. Ann Neurol 1988;3:371–9
13. Ksiezak-Reding H, Davies P, Yen S-H. Alz-50, a monoclonal antibody to Alzheimer's disease antigen, cross-reacts with tau proteins from bovine and normal human brain. J Biol Chem 1988;263: 7943–7
14. Nukina N, Kosik KS, Selkoe DJ. The monoclonal antibody, Alz-50, recognizes tau proteins in Alzheimer's disease brain. Neurosci Lett 1988;87:240–6
15. Lee VM-Y, Balin BJ, Otvos L Jr, Trojanowski JQ. A68: A major subunit of paired helical filaments and derivatized forms of normal tau. Science 1991;251:675–8
16. Bramblett G, Goedert M, Jakes R, Merrick S, Trojanowski JQ, Lee VM-Y. Abnormal tau phosphorylation of Ser396 in Alzheimer's disease recapitulates development and contributes to reduced microtubule binding. Neuron 1993;10:1089–99
17. Goedert M, Jakes R, Crowther RA, et al. The abnormal phosphorylation of tau protein at Ser-202 in Alzheimer disease recapitulates phosphorylation during development. Proc Natl Acad Sci USA 1993;90:5066–70
18. Hasegawa M, Morishima-Kawashima M, Tokio K, Suzuki M, Titani K, Ihara Y. Protein sequence and mass spectrometric analyses of tau in the Alzheimer's disease brain. J Biol Chem 1992;267: 17047–54
19. Goedert M, Jakes R, Crowther RA, Cohen P, Vanmechelen M, Cras P. Epitope mapping of monoclonal antibodies to the paired helical filaments of Alzheimer's disease: Identification of phosphorylation sites in tau protein. Biochem J 1994;301:871–7
20. Goedert M. Tau protein and the neurofibrillary pathology of Alzheimer's disease. Trends Neurosci 1993;16:460–5
21. Drechsel DN, Hyman AA, Cobb MW, Kirschner MW. Modulation of the dynamic instability of tubulin assembly by the microtubule-associated protein tau. Mol Biol Cell 1992;3:1141–54
22. Drubin DG, Kischner MW. Tau protein function in living cells. J Cell Biol 1986;103:2739–46
23. Wille H, Drewes G, Biernat J, Mandelkow E-M, Mandelkow E. Alzheimer-like paired helical filaments and antiparallel dimers formed from microtubule-associated protein tau in vitro. J Cell Biol 1992;118:573–83
24. Crowther RA, Olesen OF, Jakes R, Goedert M. The microtubule binding repeats of tau protein assemble into filaments like those found in Alzheimer's disease. FEBS Lett 1992;309:199–202
25. Crowther RA, Olesen OF, Smith MJ, Jakes R, Goedert M. Assembly of Alzheimer-like filaments from full-length tau protein. FEBS Lett 1992;337:135–8
26. McKhann G, Drachmann D, Folstein M, Katzman R, Price D, Stadlan EM. Clinical diagnosis of Alzheimer's disease: Report of the NINCDS-ADRDA Work Group under the auspices of Department of Health and Human Services Task Force on Alzheimer's Disease. Neurology 1984;34:939–44
27. Bondareff W, Wischik CM, Novak M, Amos WB, Klug A, Roth M. Molecular analysis of neurofibrillary degeneration in Alzheimer's disease: An immunohistochemical study. Am J Pathol 1990;37:711–23
28. Puchtler H, Sweat F. Congo red as a stain for fluorescence microscopy of amyloid. J Histochem Cytochem 1965;13:693–715
29. Bondareff W, Harrington C, Wischik CM, Hauser DL, Roth M. Immunohistochemical staging of neurofibrillary degeneration in Alzheimer's disease. J Neuropathol Exp Neurol 1994;53:158–64
30. Lichtenberg-Kraag B, Mandelkow E-M, Biernat J, et al. Phosphorylation-dependent epitopes of neurofilament antibodies on tau protein and relationship with Alzheimer tau. Proc Natl Acad Sci USA 1992;89:5384–8
31. Goedert M, Spillantini MG, Jakes R. Localization of the Alz-50 epitope in recombinant human microtubule-associated protein tau. Neurosci Lett 1991;126:149–54
32. Ueda K, Masliah E, Saitoh T, Bakalis L, Scoble H, Kosik KS. Alz-50 recognizes a phosphorylated epitope of tau protein. J Neurosci 1990;10:3295–304
33. Goedert M, Spillantini MG, Jakes R, Rutherford D, Crowther RA. Multiple isoforms of human microtubule-associated protein tau: Sequences and localisation in neurofibrillary tangles of Alzheimer's disease. Neuron 1989;3:519–26
34. Goedert M, Jakes R, Spillantini MG, et al. Tau protein in Alzheimer's disease. Biochem Soc Trans 1995;23:80–5
35. Kosik KS, Orecchio LD, Binder I, Trojanowski JQ, Lee VM-Y, Lee G. Epitopes that span the tau molecule are shared with paired helical filaments. Neuron 1988;1:817–25
36. Hagestedt T, Lichtenberg B, Wille H, Mandelkow E-M, Mandelkow E. Tau protein becomes long and stiff upon phosphorylation: Correlation between paracrystalline structure and degree of phosphorylation. J Cell Biol 1989;109:1643–51
37. Matsuo ES, Shin R-W, Billingsley ML, Van deVoorde A, O'Connor M, Trojanowski JQ, Lee VM-Y. Biopsy-derived adult human brain tau is phosphorylated at many of the same sites as Alzheimer's disease paired helical filament tau. Neuron 1994;13:989–1002

38. Watanabe A, Hasegawa M, Suzuki M, et al. In vivo phosphorylation sites in fetal and adult rat tau. J Biol Chem 1993;268: 25712–17
39. Wischik CM, Lai R, Edwards PC, et al. Quantitative analysis of tau protein in paired helical filament preparation. Neurobiol Aging 1995 (in press)
40. Lai RYK, Gertz H-J, Wischik DJ, et al. Examination of phosphorylated tau protein as a PHF-precursor at early stage Alzheimer's disease. Neurobiol Aging 1995 (in press)
41. Crowther RA. Tau protein and paired helical filaments of Alzheimer's disease. Curr Opin Struct Biol 1993;3:202–6
42. Biernat J, Gustke N, Drewes G, Mandelkow E-M, Mandelkow E. Phosphorylation of Ser 272 strongly reduces binding of tau to microtubules: Distinction between PHF-like immunoreactivity and microtubule binding. Neuron 1993;11:153–63
43. Alonson A del C, Zaidi T, Grundke-Iqbal I, Iqbal K. Role of abnormally phosphorylated tau in the breakdown of microtubules in Alzheimer disease. Proc Natl Acad Sci USA 1994;91:5562–6
44. Iqbal K, Zaidi T, Wen GY, Grundke-Iqbal I, Merz PA, Shaikh SS, Wisniewski HM. Defective brain microtubule assembly in Alzheimer's disease. Lancet 1986;2:421–6
45. Trojanowski JQ, Lee VMY. Paired helical filament tau in Alzheimer's disease. The kinase connection. Am J Pathol 1994;144: 449–53
46. Harada A, Oguchi K, Okabe S, et al. Altered microtubule organization in small-calibre axons of mice lacking tau protein. Nature 1994;369:488–91

Received March 27, 1995
Accepted May 1, 1995